



# A fully automated procedure for the parallel, multidimensional purification and nucleotide loading of the human GTPases KRas, Rac1 and RalB



Christopher H. Gray<sup>a,\*</sup>, Jennifer Konczal<sup>a</sup>, Mokdad Mezna<sup>a</sup>, Shehab Ismail<sup>b</sup>, Justin Bower<sup>a</sup>, Martin Drysdale<sup>a</sup>

<sup>a</sup> Drug Discovery Program, CRUK Beatson Institute, Garscube Estate, Switchback Road, Glasgow, G61 1BD, UK

<sup>b</sup> CRUK Beatson Institute, Garscube Estate, Switchback Road, Glasgow, G61 1BD, UK

## ARTICLE INFO

### Article history:

Received 8 December 2016

Received in revised form

26 January 2017

Accepted 26 January 2017

Available online 28 January 2017

### Keywords:

Human small GTPases

Histidine tag

FPLC

Automated protein purification

Multidimensional purification

Parallel purification

Protein conditioning

Nucleotide exchange

## ABSTRACT

Small GTPases regulate many key cellular processes and their role in human disease validates many proteins in this class as desirable targets for therapeutic intervention. Reliable recombinant production of GTPases, often in the active GTP loaded state, is a prerequisite for the prosecution of drug discovery efforts. The preparation of these active forms can be complex and often constricts the supply to the reagent intensive techniques used in structure base drug discovery. We have established a fully automated, multidimensional protein purification strategy for the parallel production of the catalytic G-domains of KRas, Rac1 and RalB GTPases in the active form. This method incorporates a four step chromatography purification with TEV protease-mediated affinity tag cleavage and a conditioning step that achieves the activation of the GTPase by exchanging GDP for the non-hydrolyzable GTP analogue GMPPnP. We also demonstrate that an automated method is efficient at loading of KRas with mantGDP for application in a SOS1 catalysed fluorescent nucleotide exchange assay. In comparison to more conventional manual workflows the automated method offers marked advantages in method run time and operator workload. This reduces the bottleneck in protein production while generating products that are highly purified and effectively loaded with nucleotide analogues.

© 2017 The Authors. Published by Elsevier Inc. This is an open access article under the CC BY-NC-ND license (<http://creativecommons.org/licenses/by-nc-nd/4.0/>).

## 1. Introduction

Cellular processes rely on small GTPases for the regulation of diverse, key signalling cascades and networks. Signal transduction relies on the activation of these GTPases when the bound nucleotide is swapped from GDP to the more abundant GTP through interaction with Guanine Nucleotide Exchange Factors (GEFs) [1,2]. The small GTPase KRas is the most frequently mutated gene in cancer and is a critical driver and negative prognostic factor for major presentations including colorectal, pancreatic and non small cell lung cancer [3]. Rac1 is often implicated in cancer progression, promoting angiogenesis and metastasis [4]. Similarly, the Ral GTPases promote tumorigenesis with RalB emerging as a particular driver of invasion and metastasis [5]. As a consequence, the small GTPases are established as strongly validated targets for

therapeutic intervention.

Historically, efforts to target GTPases with small molecules have proved extremely difficult with several declaring these proteins to be undruggable. However, persistence on these high value targets has led to recent encouraging progress, including the direct targeting of mutant KRas [6]. A series of small molecules have been characterized that directly bind KRas to inhibit SOS1 catalysed nucleotide exchange *in vitro* [7,8]. Other small molecules covalently interact with the KRas G12C mutant and show modulation of KRas G12C in a cellular setting by blocking nucleotide exchange and trapping the KRas in the inactive GDP form [9]. Additionally, some cyclic peptides have been reported to affect KRas, blocking protein-protein interactions with downstream effectors [10].

As a consequence of this high level of target validation in disease, and encouraging signs of tractability, the small GTPases are once again the subject of intensifying drug discovery efforts. These programs often require significant amounts of purified recombinant proteins to prosecute their programs, and often this includes

\* Corresponding author.

E-mail address: [c.gray@beatson.gla.ac.uk](mailto:c.gray@beatson.gla.ac.uk) (C.H. Gray).

GTPase protein manipulated to be in various nucleotide loaded forms.

Protein production can become an early bottleneck in the drug discovery pipeline and continual, diverse efforts seek to increase efficiency and minimize constraints [11]. Laboratory scale protein production must routinely generate multi-milligram quantities of highly purified targets for NMR, protein crystallography and other material intensive techniques. This can be a time consuming and labor intensive process. Recently released FPLC purification systems provide easier access to multidimensional chromatography that can link sequential purification steps to provide an automated process requiring much less operator intervention [12–14]. The capacity of the most advanced systems allows for parallel purification of multiple proteins in multidimensional configurations offering significant enhancements in the process throughput.

We have developed a new expression vector with an N-terminal double His<sub>8</sub> affinity tag that is highly efficient in the production of recombinant GTPases. The GTPases are purified by four FPLC steps interspersed with affinity tag cleavage by Tobacco Etch Virus protease and the exchange of GDP to alternative nucleotides, thus producing highly purified active or modified GTPases. A comparison of this automated method with a more conventional manual FPLC workflow demonstrates effective protein production with a substantial reduction in run times and workload.

## 2. Material and methods

### 2.1. Creation of the pBDDP-SPR3 expression vector and cloning of GTPases

In order to satisfy the technical requirements of downstream applications, a novel expression vector was designed that affords recombinant protein expression with an N-terminal “double His<sub>8</sub>” affinity tag [15] that includes two repeat octa-histidine motifs separated by a flexible 28mer linker. (More extensive histidine tags have proven essential for stable metal affinity immobilization in techniques such as surface plasmon resonance (SPR) [16].) The tag includes an ENLYFQG sequence to allow removal on cleavage by Tobacco Etch Virus (TEV) protease (Fig. 1a). The cassette sequence, including a bespoke multiple cloning site, was gene synthesized (Genewiz Inc) and cloned into the NcoI and XhoI sites of pET28a (Novagen) (Fig. 1b) to create pBDDP-SPR3. Three cDNAs encoding the G-domains of human KRas 4B (1–169), Rac1 (2–177) and RalB (12–186) were synthesized with codon optimisation for *E. coli* expression and each cloned to the BamHI and XhoI sites of pBDDP-SPR3 to generate three expression constructs. Correct insertions of the tag-MCS insert to pET28a and the GTPase cDNAs to pBDDP-SPR3 were confirmed by DNA sequencing.

### 2.2. Expression of the CDC25 GEF domain of SOS1 and G-domains of KRas 4B, Rac1 and RalB in pBDDP-SPR3

Plasmids were transformed into the BL21 (DE3) pLysS strain of *E. coli* (Merck Millipore) and the transformed cells were cultured overnight at 37 °C in Luria Bertani broth supplemented with 30 µg/ml kanamycin sulfate (Melford Laboratories Ltd). A volume of 20 ml this overnight starter culture was used to inoculate each of 6 × 1 L of Luria Bertani broth supplemented with 30 µg/ml kanamycin sulfate. When the OD<sub>600</sub> reached approximately 0.8, protein expression was induced by the addition of IPTG to 0.5 mM and expression was allowed to proceed for 16 h at 18 °C. Cells were harvested by centrifugation at 4000 rpm for 15 min. Cell pellets were resuspended in 50 ml lysis buffer (50 mM Tris HCl pH 7.5, 300 mM NaCl, 100 µg ml<sup>-1</sup> PMSF) and snap frozen in liquid nitrogen prior to storage at –80 °C.

### 2.3. Small scale validation the soluble expression

In order to confirm successful soluble expression prior to large scale purification, culture samples were collected immediately prior to IPTG induction and at the time of harvesting. A 1 ml sample of culture were harvested by centrifugation and resuspended in 100 µl of TBS buffer supplemented with 1 µl of endonuclease (BaseMuncher, Expediton). In order to achieve ideal loading concentrations for SDS-PAGE, the correct cell sample volume (in microliters) was determined as 8.5 × OD<sub>600</sub>. Total cell protein was applied directly to SDS-PAGE to visualize over-expression of the target.

In addition, a 40 ml volume of culture was centrifuged at 4000 rpm for 15min and the pellet resuspended in 300 µl of 50% TBS buffer, 50% Bugbuster® (Merck Millipore) and 2 µl of BaseMuncher endonuclease (Expediton). Lysis was achieved by repeated freeze thaw cycles and the lysate was clarified in a microcentrifuge at 13,000 rpm for 10 min. The clarified lysate was applied to a spin column containing 100 µl of Cobalt-NTA (CoNTA) resin (Agarose Bead Technologies). Protein was applied to the resin and washed four times with 500 µl of TBS supplemented with 10 mM imidazole and the washed beads were finally resuspended in 70 µl of TBS. Immobilized protein was visualized by directly applying 10 µl of the CoNTA beads to SDS-PAGE.

### 2.4. Purification of H8-H8-SOS1 564-1049

H8-H8-SOS1 564–1049 was purified by immobilized metal affinity chromatography (IMAC) on 5 ml HisTrap FF crude column equilibrated in Buffer A (50 mM TrisHCl pH7.5, 300 mM NaCl, 10 mM Imidazole). The column was washed with Buffer A supplemented with 30 mM imidazole and the protein was eluted by a two phase linear gradient between IMAC A and IMAC B (50 mM TrisHCl pH7.5, 300 mM NaCl, 1M Imidazole), applying 4%–50% IMAC Buffer B over 10 column volumes (50 ml) and 50%–100% IMAC Buffer B over 5 column volumes (25 ml). SOS1 was further purified on a size exclusion chromatography (SEC) 26/60 S75 Superdex Prep Grade column in Buffer D (20 mM TrisHCl pH7.5, 100 mM NaCl).

### 2.5. Purification of GTPases

Cell pellets from 6 L of culture were thawed in a 35 °C water bath, lysed by ultra-sonication and the lysates clarified by centrifugation at 20,000 rpm for 1 h. Protein purification and conditioning was performed on an ÄKTA AVANT 25 FPLC operated by Unicorn 7 software (GE Healthcare). The configuration of the ÄKTA system was as per the manufacturer's standard with the addition of a second sample inlet valve, to increase input capacity, and a loop valve to store and deliver reagents for nucleotide exchange.

Each GTPase was purified by a sequence of chromatography steps (all columns from GE Healthcare). Initial capture was achieved by IMAC on 5 ml HisTrap FF crude columns using the same buffers and strategy described for the purification of H8-H8-SOS1 564–1049. Eluted protein was collected as either 2 ml fractions in the fraction collector or in a 50 ml tube via the outlet valve, depending on the protocol used. GTPases were buffer exchanged via a 26/10 desalting (DS) column into Buffer C (20 mM Tris HCl pH7.5, 300 mM NaCl, 3 mM DTT). The double His<sub>8</sub> tag was then removed by incubation with H8-TEV S219V protease [17] (produced as previously described [18]) at a 1:50 w/w ratio for a minimum of 6 h at 4 °C. Proteins were then applied to a size exclusion chromatography (SEC) 26/60 S75 Superdex Prep Grade column in Buffer D (20 mM Tris HCl pH7.5, 100 mM NaCl) with a 5 ml HisTrap FF crude column attached at the SEC column outlet to trap any

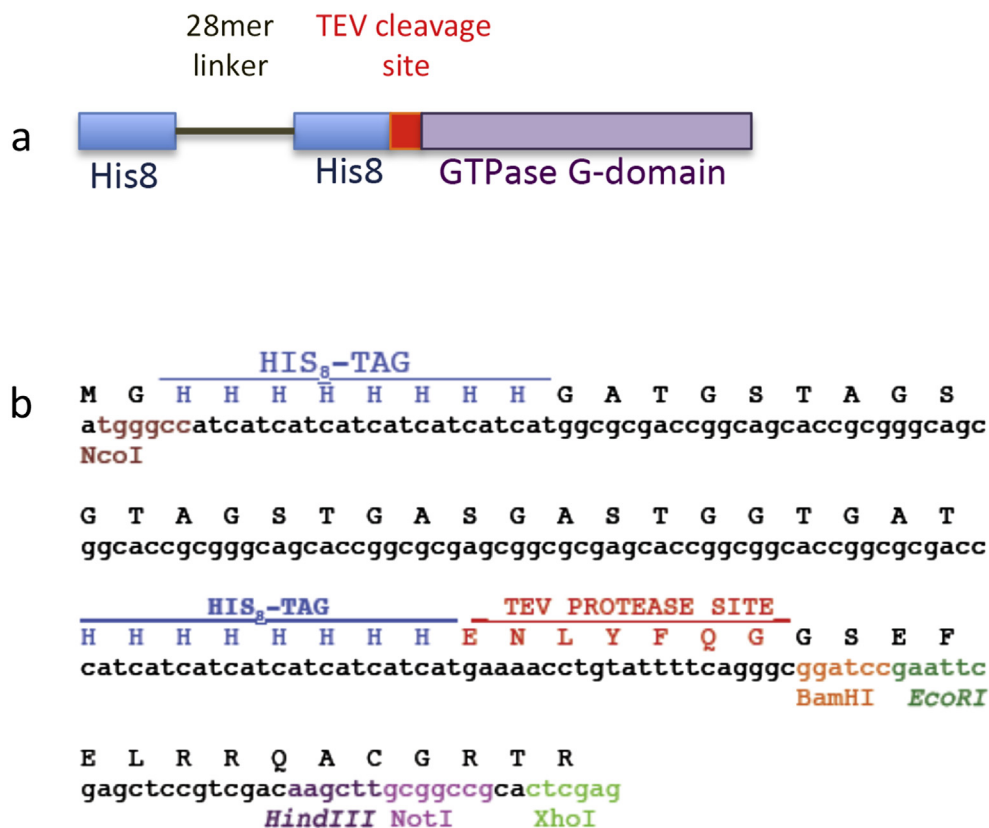


**Fig. 1. The pBDDP-SPR3 expression vector.** (A) General structure of the recombinant protein produced from pBDDP-SPR3 showing two N-terminal His<sub>8</sub> tags separated by a 28 amino acid linker followed by a TEV cleavage site. (B) The sequence and features of the pBDDP-SPR3 tag and multiple cloning site: This cassette was designed with flanking NcoI and XhoI sites to allow cloning into pET28a. This resulted in the removal of the entire pET28a tag and MCS region and replacement with the BDDP-SPR3 insert.

uncleaved GTPase and the H8-TEV S219V. GTPases were then conditioned by a nucleotide exchange reaction, and the protein was separated from excess unbound nucleotide by a 26/10 desalting column in Buffer E (10 mM Tris HCl pH7.5, 50 mM NaCl, 2 mM MgCl<sub>2</sub>).

## 2.6. Nucleotide exchange

The exchange of GDP (guanosine diphosphate) for the nucleotide analogues was achieved by methods adapted from Scherer et al. [19]. For the exchange of GDP to GMPPnP (guanosine 5'-[β,γ-imido]triphosphate), an appropriate volume (typically 3 ml) of 10× exchange buffer (containing at minimum five-fold molar excess of GMPPnP; 2M (NH<sub>4</sub>)<sub>3</sub>PO<sub>4</sub>, 1 mM ZnCl<sub>2</sub>, 5 mM GMPPnP) was delivered to the GTPase. This was achieved by either an automated step, supplying reagent from a reservoir attached to a loop valve, or by manual addition. Also, 10U per milligram of alkaline phosphatase agarose (Roche) was included by either pre-positioning in the collection tube for the SEC output, or by manual addition. GDP to GMPPnP nucleotide exchange was performed to completion on incubation for a minimum of 4 h at 4 °C.

KRas was loaded with mantGDP by incubating the protein with a molar excess of nucleotide (800 μM) and 10 mM EDTA for 2 h at 4 °C. Reactions were then supplemented with 10 mM MgCl<sub>2</sub> and incubated for a further 1 h at 4 °C prior to desalting into Buffer E. Automation of mantGDP loading was achieved by positioning of a 10× stock solution, of 8 mM mantGDP plus 50 mM EDTA, in a reservoir attached to position 1 of the loop valve. Similarly, MgCl<sub>2</sub> was delivered from a 200 mM stock attached to loop valve position 2.

## 2.7. Workflow configurations

GTPase purifications were performed either as single runs or as parallel batches where all three targets were processed in each step using the Unicorn 7 software “scouting” functionality.

In addition, workflows were designated as either “manual” or “automated”. Manual workflow involved conventional practices where proteins were applied to a single chromatography technique and purified material was subsequently collected from the ÄKTA fraction collector by the operator. The protein was then pooled and prepared for application to the next step in the production procedure, including manual addition of protease or nucleotide loading reagents.

Automated workflow made use of the Unicorn software’s “method queuing” functionality where all sequential chromatography steps can be programmed to run in sequence with no operator intervention. The desired peaks from automated purification steps were sent to 50 ml tubes via the ÄKTA outlet valve. Sample inlet lines were pre-positioned in these tubes to allow onward delivery to downstream steps. H8-TEV S219V and alkaline phosphatase agarose were pre-positioned in the appropriate intermediate tubes during the run setup. Other reagents for nucleotide exchange buffer were delivered to the pool of protein from a 10 ml sample loop attached to an ÄKTA loop valve.

## 2.8. HPLC assessment of GMPPnP loading

A 500 μl sample of protein at approximately 50 μM was heated to 95 °C for 2 min to denature the protein and release bound nucleotide. The precipitated protein was removed by centrifugation

at 13,000 rpm for 2 min and the supernatant was loaded into a HPLC auto-sampler. Analysis was carried out on a Shimadzu HPLC using a Xselect<sup>®</sup> C18 CSH 2.5  $\mu\text{m}$  column (4.6 mm  $\times$  7.5 cm) (Waters) running at 1.5 ml per minute in a buffer of 100 mM  $\text{K}_3\text{PO}_4$  pH6.5, 10 mM tetra-butyl-ammonium-bromide and 7.5% acetonitrile. Detection of nucleotide was achieved by monitoring absorbance at 254 nm and the nucleotide was identified with reference to 100  $\mu\text{M}$  GDP or GMPPnP standards.

### 2.9. SOS1 catalysed nucleotide exchange of KRas

A fluorescent based nucleotide exchange assay was performed using mantGDP loaded KRas 1–169. This assay monitors the quenching of mantGDP fluorescence as it is displaced from KRas by  $\text{GTP}\gamma\text{S}$  on interaction with the GEF SOS1. KRas 1–169 (mantGDP loaded) and SOS1 (564–1049) were mixed in a black, 96 well plate to concentrations of 500 nM and 100 nM respectively and a volume of 23  $\mu\text{l}$ . Samples were mixed on a shaking platform for 2 min and baseline fluorescence was established by an Infinite M1000 Pro fluorimeter (Tecan) (excitation wavelength, 360 nm; emission wavelength 430 nm). The reaction was initiated by the addition and mixing of 2  $\mu\text{l}$  of  $\text{GTP}\gamma\text{S}$  to a final concentration of 200  $\mu\text{M}$ . Nucleotide exchange was measured by the decrease in emission at 430 nm over a period of 90 min measuring every 60 s.

## 3. Results

### 3.1. Validation of expression of soluble human GTPases from pBDDP-SPR3

As part of a workflow optimisation program we decided to introduce routine small scale analysis of expression cultures prior to protein purification of the batch. In this way we would validate batches for onward purification or discard batches that were unsatisfactory and inefficient for further work. We determined the level of recombinant protein by noting the appearance of the target in expression cultures following IPTG induction, and confirming the presence of soluble GTPase that could be purified by IMAC resins.

Cultures were incubated and induced as per our most common laboratory protocols, and these proved satisfactory for recombinant expression. A small sample of cells were harvested at the time of induction (T = 0) and at harvesting (endpoint) and resuspended in TBS buffer. A simple formula related culture  $\text{OD}_{600}$  to the volume of resuspension buffer to generate a sample that gave an appropriate concentration of total cell protein on an SDS-PAGE gel. In this way we could typically ensure a gel lane of well separated bands with a clear indication of the overexpressed target GTPase. In the vast majority of expression cultures the G-domains of KRas, Rac1 and RalB expressed well in pBDDP-SPR3. In addition an acceptably clean small scale Co-NTA purification confirmed the presence of all three GTPases as soluble proteins at appropriate molecular weights and with intact His-tags, thus confirming suitability of the batches for onward FPLC purification (Fig. 2).

### 3.2. Design of an automated, multidimensional, parallel production strategy

In order to increase throughput and productivity we devised a strategy for the parallel, automated production of several activated GTPases by multi-dimensional chromatography. Purification was achieved using standard enrichment and purification approaches, principally IMAC and SEC. Desalting columns were incorporated to facilitate buffer exchange. In our hands, these GTPases aggregate after sufficient exposure to imidazole, resulting in a loss of yield and quality. Buffer was exchanged immediately after IMAC to ensure no

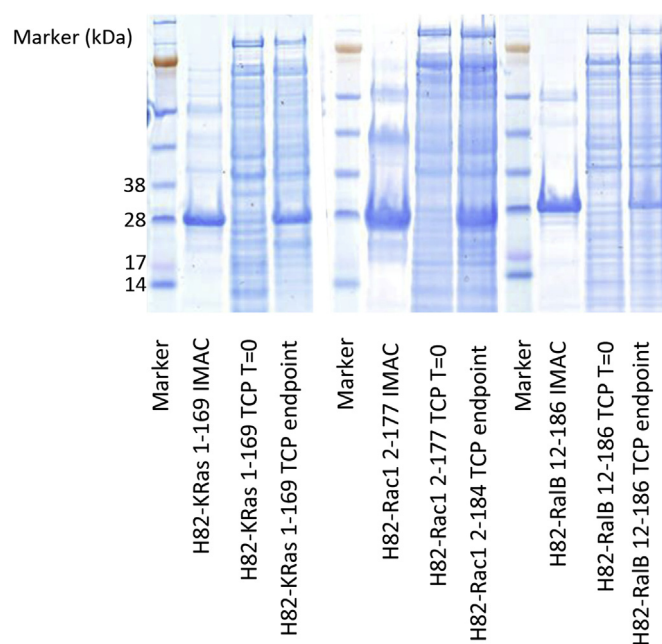


**Fig. 2. Small Scale expression analysis from pBDDP-SPR3 constructs.** GTPases were expressed in the BL21 (DE3) pLysS strain of *E. coli* in Luria Bertani broth supplemented with 30  $\mu\text{g}/\text{ml}$  kanamycin sulfate. A 1 ml sample of cells was collected before induction and at the time of cell harvesting. This allowed the assessment of total cell protein by SDS-PAGE, and the visualisation of over-expressed target protein. A 40 ml sample of expression culture was applied to a small scale CoNTA IMAC purification to demonstrate the presence of soluble his-tagged protein. (As reported by others, CoNTA spin column purification has proved particularly useful in this respect and gives a consistently clear indication of levels and integrity of recombinant proteins [20].) In all three cases there was significant soluble expression of the GTPase allowing progression to FPLC scale purification (H<sub>8</sub>-H<sub>8</sub>-KRas 1–169, 24.8 kDa; H<sub>8</sub>-H<sub>8</sub>-Rac1-2-177, 26.2 kDa; H<sub>8</sub>-H<sub>8</sub>-RalB, 25.5 kDa).

imidazole persisted during the 6 h incubation with TEV protease. A second buffer exchange was required following nucleotide loading, as the GMPPnP is applied at significant molar excess so the unbound nucleotide must be removed from the final product and exchange buffer conditions are not ideal for downstream applications. Overall, the sequence of the workflow was IMAC->Desalting->TEV cleavage (6 h pause)->S75 SEC\*->Nucleotide exchange (4 h pause)->Desalting (panel, Fig. 3). (\*SEC had a 5 ml nickel column in line to trap uncleaved product and TEV protease.)

For tag cleavage, TEV protease was pre-placed in the tube allocated to receive the appropriate desalting column elution peak. To produce active GTPases the nucleotide was exchanged from GDP to a GTP analogue as the protein emerges from *E. coli* in the inactive GDP bound form. In our workflow we incorporated the nucleotide exchange of GDP with the non-hydrolyzable GMPPnP (or other required analogue) following elution from the SEC column. Alkaline phosphatase agarose reagent was pre-placed in the tubes receiving the material for nucleotide exchange. A 10 $\times$  exchange buffer, containing the concentrated ammonium sulfate and GMPPnP, was held apart from the agarose until required. (The high salt concentration of the 10 $\times$  buffer eliminated the phosphatase activity and it was preferable to keep the GMPPnP and phosphatase separate in case some low level hydrolysis did occur.) A loop valve was added to the AKTA configuration to hold a reservoir of 10 $\times$  exchange buffer stock. Following the completion of the SEC column, a short method was included in the method queue to deliver 3 ml of 10 $\times$  exchange buffer to the protein in the waiting tubes. This material was applied at a flow rate of 10 ml per minute and this successfully agitated the phosphatase agarose in the tube to disperse it throughout the



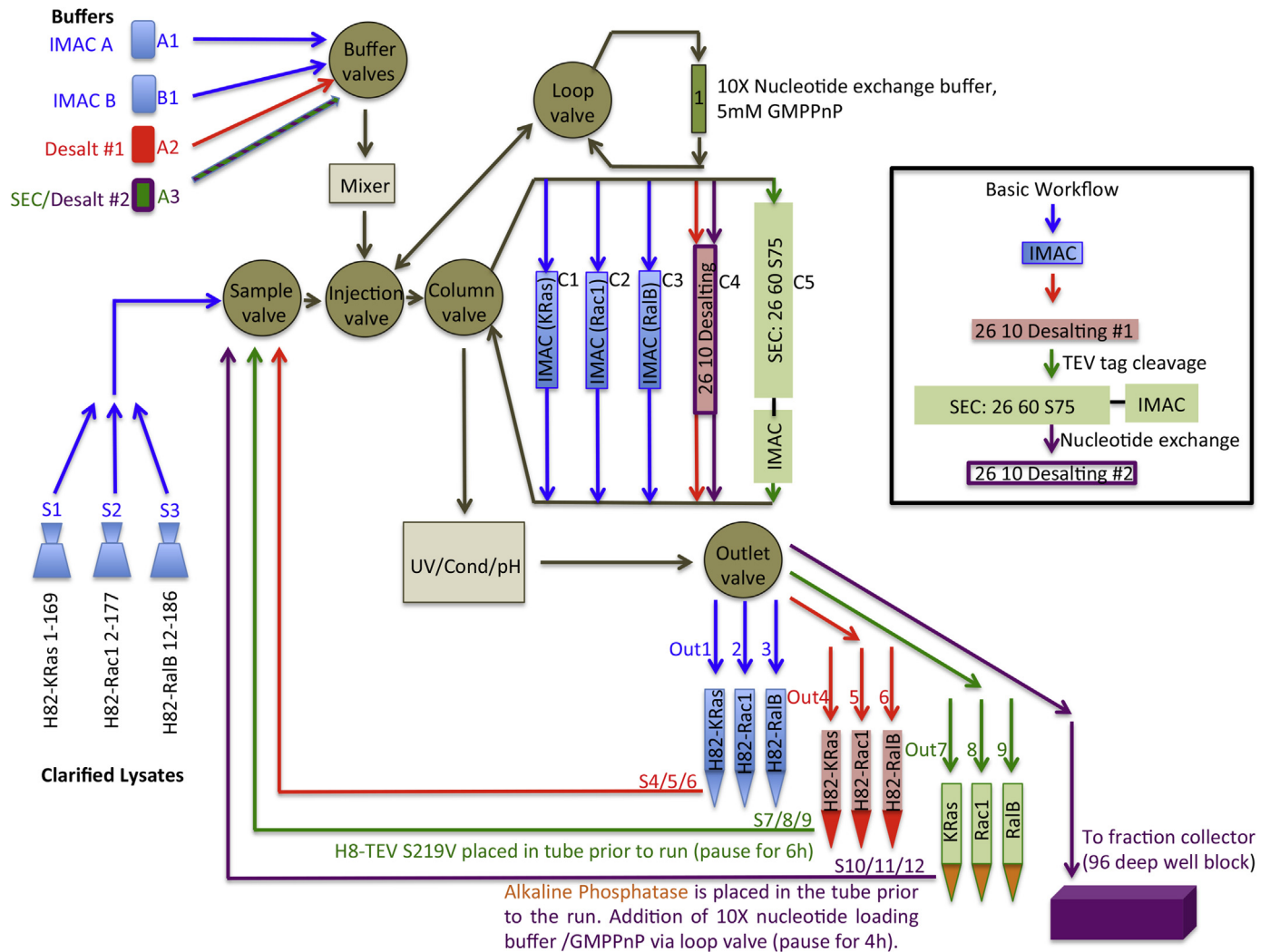


**Fig. 3. Multidimensional schematic for parallel GTPase production.** An example flow diagram of the multidimensional purification configuration on the ÄKTA AVANT 25 system for the parallel purification of three active, GMPPnP loaded GTPases. Flow of samples to and from the columns was achieved using tubing connected to sample inlet or outlet valves respectively. Each purification included four column steps and integrated both TEV protease tag cleavage and a nucleotide loading reaction. GTPases were purified on a dedicated 5 ml HisTrap FF IMAC column followed by a 26/10 desalting column to remove imidazole. H8-TEV S219V protease then cleaved the tag from the GTPases during a 6 h incubation. Cleaved proteins were purified further on a 26/10 S75 Superdex Prep Grade Column with a 5 ml HisTrap FF column attached downstream (to capture H8-TEV S219V and any un-cleaved material). Finally the protein was delivered to an aliquot of alkaline phosphatase agarose. The 10 $\times$  nucleotide exchange buffer, containing an excess of GMPPnP, was delivered to from a reagent reservoir connected to a loop valve. Nucleotide loading was allowed to proceed for 4 h and a final 26/10 desalting run removed excess nucleotide and collected the material in the integrated fraction collector prior to delivery. All intermediate product collection, protease reactions and nucleotide loading was performed in pre-positioned 50 ml tubes. GE Healthcare Unicorn 7.0 software was programmed with a series of “scouting” runs and “method queues” to automatically schedule all steps in the production workflow running in sequence and without any user intervention.

mixture. (Similarly, reagents for the loading of KRas with mantGDP were held in two 10 ml sample loops on the loop valve and appropriate volumes delivered to initiate and stabilise exchange.) TEV protease, exchange buffer, and nucleotide exchange reagents were applied at concentrations sufficient to achieve the desired modification of the maximum anticipated protein yield. As there was some variation in yields between replicate batches, it was not possible to be precise with ratios but we observed no negative effects on the product on occasions where the modifying reagents were in unnecessary excess.

The multi-dimensional flowpath and run scheduling were established using the method queuing functionality in GE Healthcare's Unicorn software incorporating pauses to allow for tag cleavage or nucleotide exchange. The parallel purification of multiple GTPases used the Unicorn 7 scouting option, where the processing of several samples can be included in the same

chromatography method. To prosecute the three production runs, an integrated multidimensional flow path was established utilising 12 ports of the extended sample inlet valve, 5 ports of the column selection valve, 9 ports of the outlet valve and the fraction collector (Fig. 3). All intermediate products were successfully collected in 50 ml tubes via the outlet valve ensuring the appropriate peak was selected and positioned for onward processing.

In order to restrain the early sample volume, the elution gradient from the IMAC was steep to compress the volume of that first elution peak and restrain requirements to one SEC column run per GTPase. However, sample dilution was noted through the run and it was common to run two final desalting columns after nucleotide exchange to process the entire final sample volume.

### 3.3. Parallel purification and activation using the multidimensional system

An example of the set of chromatograms is presented in Fig. 4, illustrating the purification of tag cleaved, activated KRas 1–169. A robust workflow was achieved following trial and optimisation that allowed the successful isolation of all the GTPase targets. Proteins isolated by both automated and manual methods exhibited mobility on SDS-PAGE consistent with a species cleaved by TEV protease. Comparison of products from the automated and manual workflows showed comparable levels of purity on coomassie stained gels. However, using silver stain revealed that the material from the multidimensional workflow appeared to be marginally more purified (Fig. 5).

An initial concern was that stringent peak recognition parameters and rigid adherence to injection volumes within runs would result in a reduced yield from the automated method versus the manual approach. Surprisingly we routinely encountered the opposite. As expected the comparative yields from the first IMAC step showed the lowest discrepancy between approaches with average outputs from both methods approximately equal ( $n = 3$ ) (Fig. 6a). However, greater losses are consistently observed with the

manual method. It would appear that a combination of extended processing time and the manipulation and transfer of intermediate products between plasticware results in more attrition than the automated approach. Marginally, the greatest point of loss is seen in the yields from the SEC column, possibly as result of increased protein aggregation following prolonged storage in the fraction collector or from manual handling. Ultimately, substantial multi-milligram quantities were obtained by all methods but the automated approach invariably returned the higher yields with the enhancement ranging between 8.5% and 16.9% when compared to the manual workflow (Table 1).

### 3.4. Nucleotide loading and SOS1 catalysed nucleotide exchange

GMPPnP status was ascertained by HPLC. Both manual and automated loading showed complete incorporation of GMPPnP in all GTPases with a positive GMPPnP peak, at amplitudes consistent with the analyzed protein concentration, and a complete absence of any signal for the GDP species (Fig. 7).

The utility of KRas 1–169 loaded with mantGDP was assessed by application in a SOS1 dependant fluorescent nucleotide exchange assay (Fig. 8a). Both methods produced loaded material that

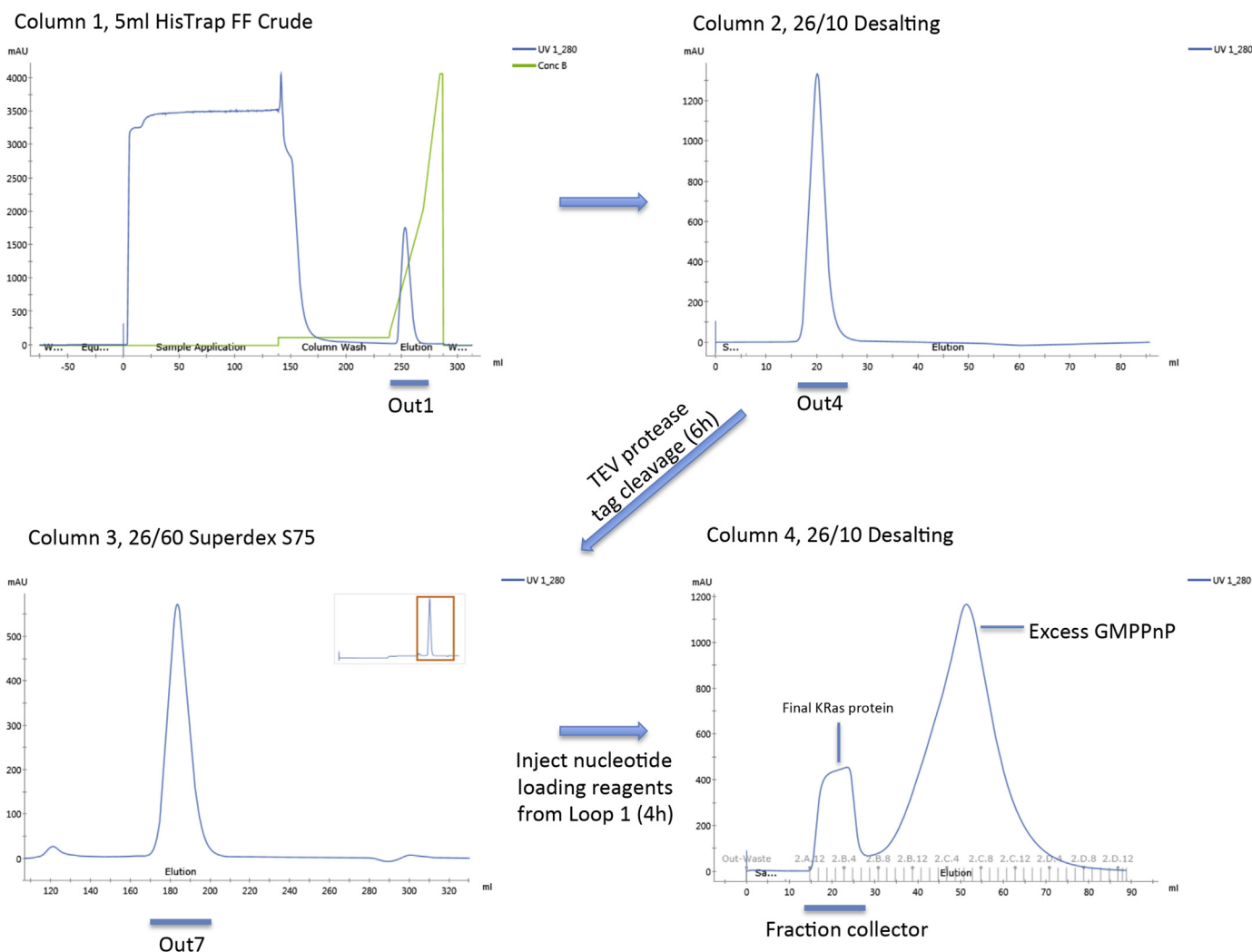


**Fig. 4.** Purification of GTPases. A typical set of chromatograms generated on the multidimensional purification of KRas 1–169 through IMAC-Desalting-TEV protease cleavage-SEC-nucleotide loading-Desalting. Prior understanding of the purification behaviour of each GTPase allowed methods to be compiled that ensured the collection of the correct elution peak via the outlet valve and the successful delivery of the product to the next column in the series.

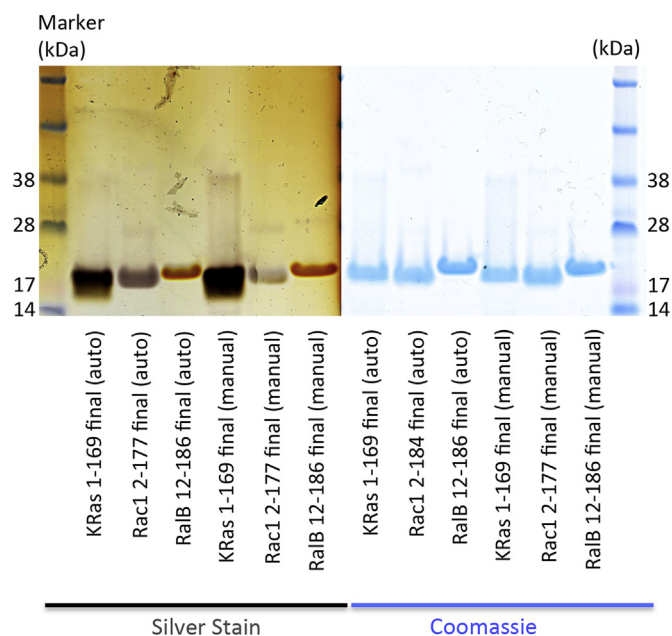


**Fig. 5.** SDS-PAGE analysis of purified proteins. A total of approximately 5  $\mu\text{g}$  ( $5 \mu\text{l}$  of  $1 \text{ mg ml}^{-1}$ ) of each protein was analyzed by SDS-PAGE and demonstrated good levels of purity and complete removal of the H8-H8- tag. Comparable purity was observed on coomassie stained gels, more sensitive analysis by silver staining suggested that there was a slightly reduced presence of minor contaminant species with proteins produced by the automated method.

**Table 1**

A comparison of final yields (mg) from each approach revealed an enhancement of between 8.5% and 16.9% through the use of the automated workflow.

|             | Automatic | Manual | Manual vs Auto |
|-------------|-----------|--------|----------------|
| KRas 1–169  | 48.0      | 39.9   | 83.1%          |
| Rac1 2–177  | 61.4      | 55.5   | 90.2%          |
| RalB 12–186 | 46.9      | 42.9   | 91.5%          |

### 3.5. Evaluation of workflow enhancements from the automated system

Often individual process steps in a manual method will complete outside routine working hours leaving the equipment idle or extending the incubation times with TEV protease or nucleotide exchange reagents. This is not the case in the automated method which has substantial time benefits compared to the manual approach. We established typical processing times for each workflow and demonstrated that the parallel purification of the three GTPases was over 29 h faster using the automated multidimensional method. When comparing the single GTPase run data, the automated preparation of a one GTPase domain almost 24 h quicker (Fig. 9). The net result is quicker delivery, increased FPLC throughput and a fresher protein product delivered to the downstream application.

## 4. Discussion

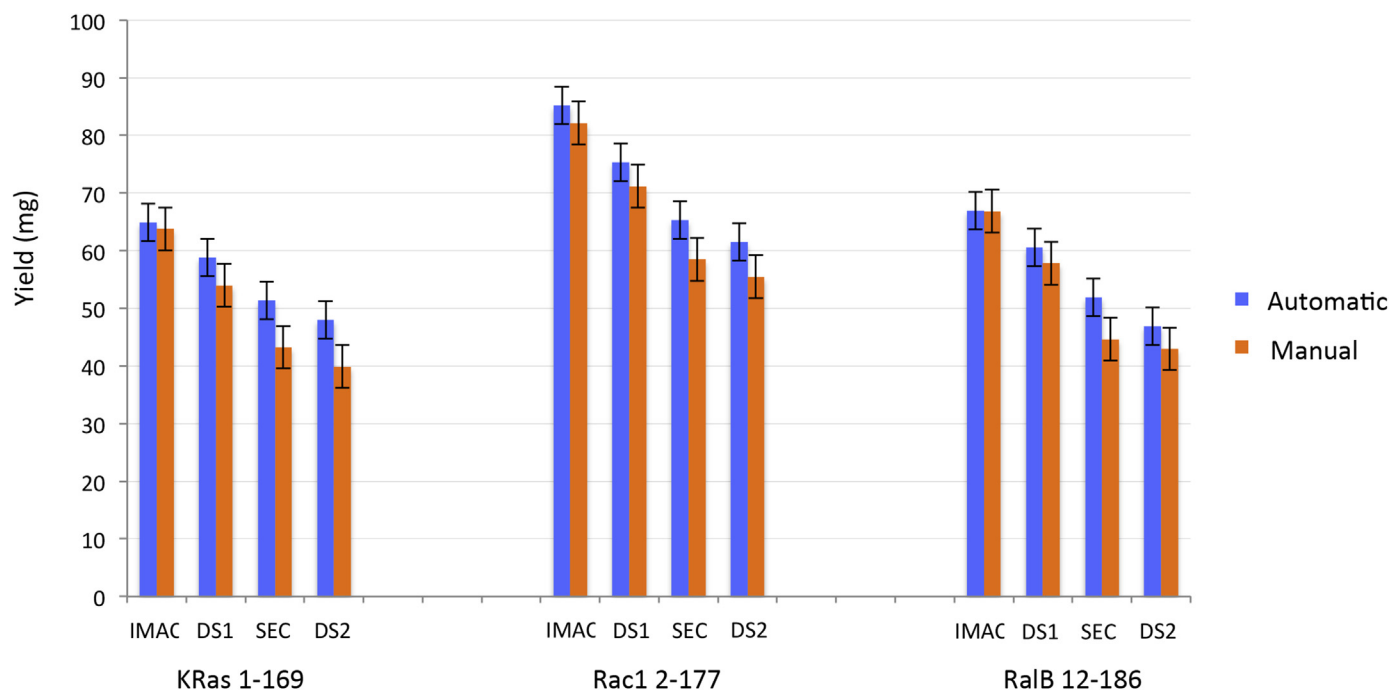


**Fig. 6.** Analysis of protein yields from automatic and manual workflows. Average yields for each column step were established for both automated and manual workflows by integrating the elution peak area using the Unicorn 7 evaluation module. Multi-milligram quantities of each GTPase were invariably produced but the automated approach consistently returned higher yields.

showed very similar exchange kinetics of SOS1 dependant exchange (automated,  $1.15 \pm 0.032 \times 10^3 \text{ sec}^{-1}$ ; manual  $1.20 \pm 0.010 \times 10^3 \text{ sec}^{-1}$ ) demonstrating that automated preparation of mantGDP loaded material was suitable for downstream applications (Fig. 8b).

Many research programs, including structure based drug discovery, utilize a lot of protein intensive techniques, such as x-ray crystallography, nuclear magnetic resonance or isothermal titration calorimetry. As a consequence it is very easy for protein production to become a rate limiting factor in the discovery process. Whilst it is

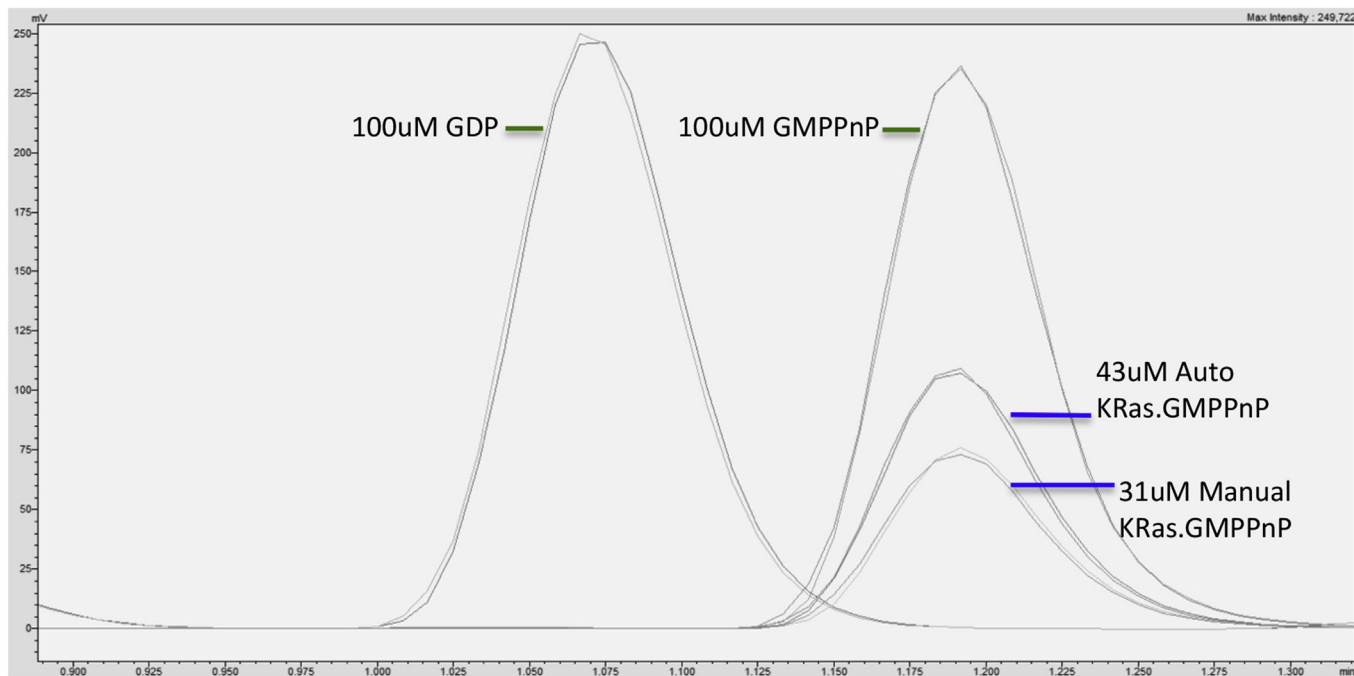


**Fig. 7. HPLC analysis of GMPPnP loading.** Analysis of the nucleotide content of purified proteins demonstrated complete exchange for GMPPnP in both manual and automated processes. A typical comparison of manual versus automatic loading of KRas 1–169 by HPLC demonstrates the sole presence of the GMPPnP species and the complete absence of GDP, at levels consistent with the concentration of the protein analyzed.

not always possible to completely eliminate this, it is always advisable to monitor bottlenecks and be mindful of opportunities to reduce or eliminate them. To achieve efficiencies in this area we decided to design a flexible, fully automated system for the parallel production of multiple activated GTPases.

We developed pBDDP-SPR3 expression vector by replacing the tag and multiple cloning site of pET28a with our own bespoke configuration. This encodes for two His<sub>6</sub> motifs, a TEV protease cleavage sequence and a simplified multiple cloning site, and offers an easy to use flexible expression vector tailored to our laboratory's activities. This vector has now been used in the successful over-expression of scores of proteins in addition to those described in this paper.

The scheduling of the purifications on FPLC systems also represented an opportunity for process optimisation. The FPLCs were inactive for significant amounts of time during the purification if the operator was committed to another task or a process step completed outside of core working hours. It was clear that a reduced requirement for frequent manual intervention could enhance throughput by potentially reducing run times, uplifting capacity and may also provide the added reproducibility and reliability that can accompany automation. By enhancing the capability of our AKTA AVANT 25 systems with extra sample inlets and a loop valve we were able to develop a parallel multidimensional process for the fully automated production of nucleotide loaded GTPases.

As the overall purification sequence between automated and manual methods was the same, there was no expectation that moving to a multidimensional system would result in an improvement in protein purity. Comparison of products on coomassie stained gels suggested that purity levels between approaches was equivalent. However silver stained gels did suggest that proteins isolated by the automated workflow may be marginally purer (Fig. 5). Any degree of improved purification may seem slight but it can have significant effects on the success and performance level of techniques like protein crystallography and

NMR.

The principal motivation for this method development was to reduce run times and there were some initial concerns that yields would be reduced as a result of incomplete sample application or peak collection. Indeed, in order to minimize sample volumes for subsequent steps, and to avoid the collection of small unwanted peaks, the criteria for peak recognition was tightly specified in the software with relatively strict requirements in terms of both peak height and slope. However, our early concerns about reduced yields did not seem to materialize, with automated processing invariably producing higher yields than the manual equivalent. It would appear that any losses incurred as a result of strict peak recognition in automation were less than losses observed by manual collection and reformatting of intermediate products.

While others have described the use of multidimensional chromatography for protein purification there is less precedent for the incorporation of protein conditioning and modification steps. By attaching a reservoir to a loop valve the method was able to deliver appropriate reagents to purified proteins and achieve a complete exchange of GDP to selected nucleotide analogues. Buffer chase steps were included to push the complete volume of exchange reagents beyond the outlet valve and into the waiting protein sample. A comprehensive recording of tubing and component dead volumes and precise chasing of the reaction reagents with buffer allowed us to confidently deliver accurate triple digit microliter volumes to intermediate proteins. This component has the potential to automate a broad range of protein conditioning events including co-factor delivery, chemical modification, and the introduction of other proteins for complex formation or the delivery of enzymes to manipulate post-translational modifications.

By far the main advantage offered by automated purification is reduced run time, with a three protein parallel GTPase purifications taking approximately 44 h in contrast to the 96 h run time of the manual workflow (Fig. 9). Indeed the run time can be compressed further when producing proteins with compatible buffer



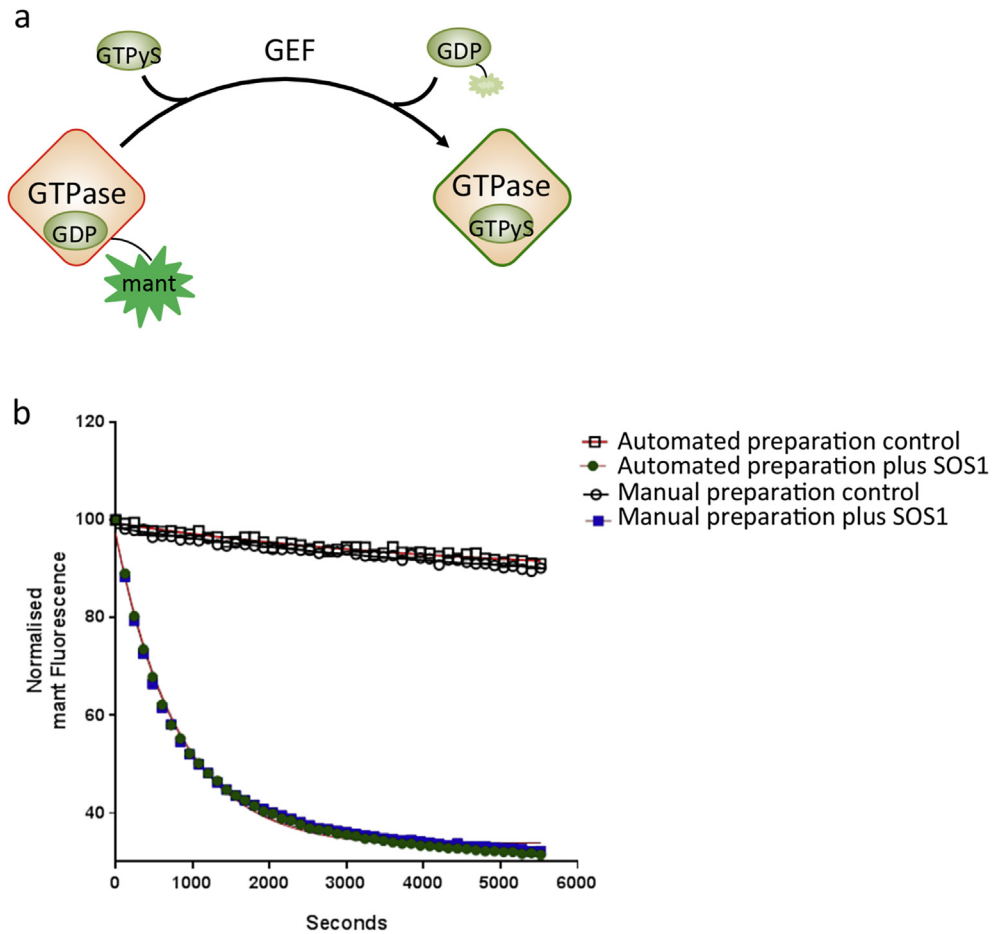


**Fig. 8. KRas/SOS1 nucleotide exchange assay.** (A) Equimolar concentrations of KRas 1–169 loaded with mantGDP by both production methods methods and applied to SOS1 catalysed nucleotide exchange which measures a quenching of mant fluorescence when it is displaced from KRas by GTP $\gamma$ S. (B) The mean rates of exchange kinetics of both preparations were almost identical (automated,  $1.15 \pm 0.032 \times 10^3 \text{ sec}^{-1}$ ; manual  $1.20 \pm 0.010 \times 10^3 \text{ sec}^{-1}$ ) demonstrating that the multidimensionally prepared mantGDP loaded KRas was suitable for downstream applications. Data was analyzed and the rates derived by fitting to a single exponential decay equation. The red line joining the data illustrates the fit. (For interpretation of the references to colour in this figure legend, the reader is referred to the web version of this article.)

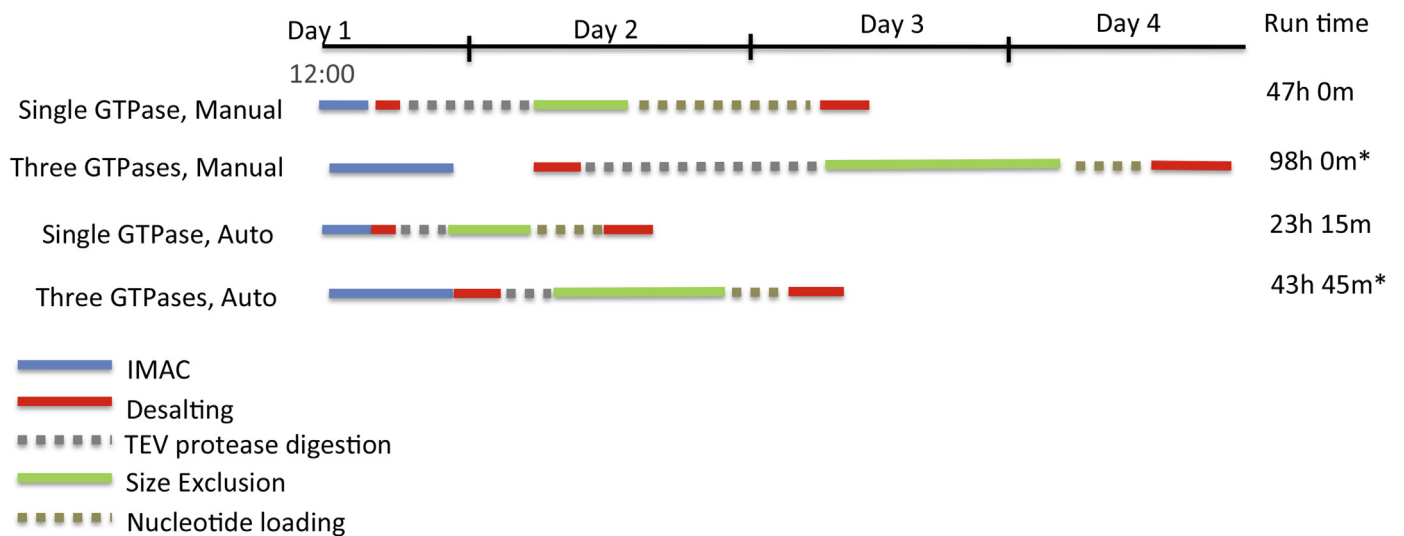


**Fig. 9. Run times for purifications by manual and automated workflows.** Recording of purification periods during both automated and manual workflows reveal substantial compression of run times using the automated method with 50% reductions in duration in both single protein and three protein parallel productions.

requirements. This allows a single equilibration of desalting and SEC columns, and then all parallel proteins can be repeatedly applied without re-equilibration between sample injections. This significantly reduces the run time - in these circumstances parallel purification of GTPases by the method described would be further reduced to only 31 h and 20 min. If it were practical to keep this system supplied with lysates when required, each FPLC could theoretically establish a throughput of 5 parallel multidimensional runs per week and an output of 15 purified, activated GTPases. Although this ideal is difficult to achieve, the methodology has greatly increased our ability to respond quickly to increases in demand while maintaining or even enhancing the yield and quality of the product. It is especially satisfying that it is now possible to incorporate a sensitive reaction, like GTPase nucleotide exchange. Both incorporation of GMPPnP and mantGDP demonstrated quality and performance consistent with KRas produced manually by either HPLC nucleotide analysis or fluorescent exchange assay (Figs. 7 and 8).

In summary, the implementation of parallel multidimensional workflows, even for relatively complex production protocols, offers busy protein production teams the opportunity to increase routine output, improve product quality and free up human resource for other tasks thus loosening the bottleneck and accelerating the discovery process.

#### Acknowledgements

We would like to thank Arron Grieg from GE Healthcare for advice on programming Unicorn 7 and the implementation of additional AKTA hardware.

#### References

- [1] A. Hennig, et al., Ras activation revisited: role of GEF and GAP systems, *Biol. Chem.* 396 (8) (2015) 831–848.
- [2] P.A. Boriack-Sjodin, et al., The structural basis of the activation of Ras by Sos, *Nature* 394 (6691) (1998) 337–343.
- [3] J.M. Ostrem, K.M. Shokat, Direct small-molecule inhibitors of KRAS: from structural insights to mechanism-based design, *Nat. Rev. Drug Discov.* 15 (11) (2016) 771–785.
- [4] H.K. Bid, et al., RAC1: an emerging therapeutic option for targeting cancer angiogenesis and metastasis, *Mol. Cancer Ther.* 12 (10) (2013) 1925–1934.
- [5] R. Shirakawa, H. Horiuchi, Ral GTPases: crucial mediators of exocytosis and tumorigenesis, *J. Biochem.* 157 (5) (2015) 285–299.
- [6] A.D. Cox, et al., Drugging the undruggable RAS: mission possible? *Nat. Rev. Drug Discov.* 13 (11) (2014) 828–851.
- [7] Q. Sun, et al., Discovery of small molecules that bind to K-Ras and inhibit Sos-mediated activation, *Angew. Chem. Int. Ed. Engl.* 51 (25) (2012) 6140–6143.
- [8] T. Maurer, et al., Small-molecule ligands bind to a distinct pocket in Ras and inhibit SOS-mediated nucleotide exchange activity, *Proc. Natl. Acad. Sci. U. S. A.* 109 (14) (2012) 5299–5304.
- [9] M.P. Patricelli, et al., Selective inhibition of oncogenic KRAS output with small molecules targeting the inactive state, *Cancer Discov.* 6 (3) (2016) 316–329.
- [10] P. Upadhyaya, et al., Inhibition of Ras signaling by blocking Ras-effector interactions with cyclic peptides, *Angew. Chem. Int. Ed. Engl.* 54 (26) (2015) 7602–7606.
- [11] T. Sugiki, T. Fujiwara, C. Kojima, Latest approaches for efficient protein production in drug discovery, *Expert Opin. Drug Discov.* 9 (10) (2014) 1189–1204.
- [12] U. Riek, et al., A versatile multidimensional protein purification system with full internet remote control based on a standard HPLC system, *Biotechniques* 46 (6) (2009) ix–xii.
- [13] Y. Kim, et al., High-throughput protein purification and quality assessment for crystallization, *Methods* 55 (1) (2011) 12–28.
- [14] Y. Kim, et al., Chapter 3. High-throughput protein purification for x-ray crystallography and NMR, *Adv. Protein Chem. Struct. Biol.* 75 (2008) 85–105.
- [15] E. Hochuli, H. Dobeli, A. Schacher, New metal chelate adsorbent selective for proteins and peptides containing neighbouring histidine residues, *J. Chromatogr.* 411 (1987) 177–184.
- [16] M. Fischer, A.P. Leech, R.E. Hubbard, Comparative assessment of different histidine-tags for immobilization of protein onto surface plasmon resonance sensorchips, *Anal. Chem.* 83 (5) (2011) 1800–1807.
- [17] D.A. Polayes, et al., Application of TEV protease in protein production, *Methods Mol. Med.* 13 (1998) 169–183.
- [18] J.E. Tropea, S. Cherry, D.S. Waugh, Expression and purification of soluble His(6)-tagged TEV protease, *Methods Mol. Biol.* 498 (2009) 297–307.
- [19] A. Scherer, et al., Crystallization and preliminary X-ray analysis of the human c-H-ras-oncogene product p21 complexed with GTP analogues, *J. Mol. Biol.* 206 (1) (1989) 257–259.
- [20] T.C. Phan, et al., Expression of caltrix in the baculovirus system and its purification in high yield and purity by cobalt (II) affinity chromatography, *Protein Expr. Purif.* 29 (2) (2003) 284–290.